Theoretical Chemistry Accounts (2020) 139:96
https://doi.org/10.1007/s00214-020-02610-2

REGULAR ARTICLE

Carboxymethylcellulose and cellulose xanthate matrices as potential adsorbent material for potentially toxic Cr^{3+}, Cu^{2+} and Cd^{2+}metal ions: a theoretical study

Davi Texeira Reis[1] · Sílvio Quintino de Aguiar Filho[1] · Carlos Guilherme Lopes Grotto[1] · Murielly Fernanda Ribeiro Bihain[1] · Douglas Henrique Pereira[1]

Received: 30 January 2020 / Accepted: 11 May 2020 / Published online: 25 May 2020

Abstract
Cellulose derivatives have been synthesized and used in various applications with emphasis on possible application in environmental remediation. In this context, the present work theoretically studied the adsorption of Cr^{3+}, Cu^{2+} and Cd^{2+} metal ions in the carboxymethylcellulose (CMC) and cellulose xanthate (CX) matrices, both derived from cellulose. From the calculations, it was possible to obtain map of electrostatic potential, frontier molecular orbitals, reactivity indices, and with these, analyses infer that the cations would interact with the CMC and CX oxygen and also with the CX sulfo group. After complexation, the results showed that the CX and CMC matrices studied have potential to be used to remove toxic metals and presented chemical adsorption and the processes occur spontaneously ($\Delta G < 0$). The topological analysis of quantum theory of atoms in molecules allowed to characterize the nature of the interaction, in which the interactions in position "b" of CMC–Cu^{2+}, CMC–Cd^{2+} and position "a" of CMC–Cd^{2+} and "a" in the complexes XC–Cu^{2+}, XC–Cd^{2+} and "b" in the XC–Cr^{3+} site (1) presented electrostatic characteristics, and the other interactions were partially covalent. The results found when compared to the study of cellulose and cellulose acetate adsorption with the same metal ions showed that the theoretical data provide insights for a possible experimental approach and use of this matrices.

Keywords Cellulose derivatives · Metal ions · DFT · QTAIM

1 Introduction

Natural biopolymers such as collagen, gelatin, chitosan and cellulose have been extensively explored in various areas of science [1]. Applications extend from the medical field, with drug delivery system, healing products, surgical implant devices [2–4], among other areas such as agriculture, filtration, hygiene and protective clothing [2, 5, 6]. Biopolymers are derived from plant, animal and microbial biomass and are considered environmentally friendly and sustainable [7–10].

Among the biopolymers found, cellulose is the most abundant natural polymer in the earth [1] and has been used as a chemical raw material for approximately 150 years [6]. It is a polysaccharide formed from repetitive D-glucose units, bonded by β(1-4)-glycoside bonds [6, 11], and its chain consists of hydroxyl groups and methanol and has an ordered structure, without side chains [6, 11]. In addition to cellulose, derivatives of this natural polymer have been synthesized and used in industry and various applications [6, 12]. Recently, our research group studied using theoretical calculations based on density functional theory (DFT) the interaction of Cr^{3+}, Cu^{2+} and Cd^{2+} metal ions in cellulose (CE) and cellulose acetate (CA) matrices [13]. The results showed that the matrices interact with the metal ions and are excellent alternatives for the removal of metal ions from effluents. In addition to cellulose acetate, other derivatives are noteworthy, such as cellulose xanthate (CX) and carboxymethylcellulose (CMC) [6].

"Festschrift in honor of Prof. Fernando R. Ornellas" Guest Edited by Adélia Justino Aguiar Aquino, Antonio Gustavo Sampaio de Oliveira Filho and Francisco Bolivar Correto Machado.

✉ Douglas Henrique Pereira
doug@uft.edu.br

[1] Chemistry Collegiate, Federal University of Tocantins, Campus Gurupi -Badejós, P.O. Box 66, Gurupi Zip Code: 77 402-970, Brazil

Xanthates are formed by the reaction of an organic substrate with carbon disulfide under caustic conditions. Like any xanthate, cellulose xanthate is insoluble in water [6, 14] and when compared to cellulose, it has higher ion exchange capacity or adsorption, which makes its use for heavy metal removal possible [15]. Carboxymethylcellulose is a cellulose derivative formed by reaction with sodium hydroxide and sodium chloroacetic acid and when introduced into the cellulose polymer, it promotes its solubility in water [16]. Its generation is facilitated by part of its easy operational process, with constant pressure and relying on reagents that are easily found, which promoted its wide use in detergent, paint, textile industries, among others [17], in addition to potential use in the removal of toxic metals.

Both derivatives may have the potential to adsorb heavy metals such as cadmium (Cd), copper (Cu) and chromium (Cr), which cause problems in aquatic environments [18–21]. Cd is a metal that has the ability to bioaccumulate to bonding with aspartate, cysteine, glutamate and histidine groups, leading to iron deficiency [22]. Cu has the ability to catalyze free radicals [23], and Cr in its ion forms is highly toxic to living things in general [24].

Given the harmful effects of toxic metals in aquatic environments and the potential use of cellulose xanthate and carboxymethylcellulose derivatives in their removal, the present work studied the interaction of the Cr^{3+}, Cu^{2+} and Cd^{2+} metal ions in CX and CMC matrices using the density functional theory and quantum theory of atoms in molecules (QTAIM) approaches.

2 Computational details

The structures of carboxymethylcellulose and cellulose xanthate (CX) have been optimized to the minimum of energy using DFT with the hybrid function M06-2X [25]. The basis set used was 6-31+G(*d*,*p*) for the atoms: C, H, S and O. For Cu^{2+}, Cd^{2+} and Cr^{3+} metal ions, the basis set LANL2DZ [25] was used. The effect of water as solvent was considered using the SMD continuous solvent model [26]. The theory level M06-2X/6-31+G(*d*,*p*)/LANL2DZ was used for all analyses. All calculations were performed using the Gaussian 09 program [27]. The representation of some molecular structures has been obtained from the Gaussview software [28].

Gibbs energy calculations are calculated following Eq. 1.

$$\Delta G = \sum G_{\mathrm{P}} - \sum G_{\mathrm{R}} \tag{1}$$

The interaction energy has been determined from Eq. 2:

$$E_{\mathrm{int}} = E_{\mathrm{complex}} - \left(E_{\mathrm{molecule}} + E_{\mathrm{metal\ ion}}\right) \tag{2}$$

where E_{int} is the energy of interaction, E_{complex} corresponds to the energy of the complex (polymer + ion), and E_{molecule} and $E_{\mathrm{metal\ ion}}$ are the energy of the isolated polymer and metal ion, respectively.

The chemical hardness (η) and softness (S) reactivity indices are calculated using the energy of the molecular orbitals HOMO and LUMO following Eqs. 3 and 4. The Koopmans theorem [29] was considered for the calculation.

$$\eta = \frac{\mathrm{LUMO} - \mathrm{HOMO}}{2} \tag{3}$$

$$S = \frac{1}{\eta} \tag{4}$$

The QTAIM analysis was realized to characterize the interactions between the metal ions and matrices [30–34]. All QTAIM analyses were performed using the AIMAll package [34].

3 Results and discussion

3.1 Structures before complexation

The interaction studies of the carboxymethylcellulose—CMC and cellulose xanthate—CX matrices with Cu^{2+}, Cd^{2+}, Cr^{3+} metallic ions were performed using two monomeric units of biopolymers. A previous study by our research group evaluated the interaction of the metal ions with the cellulose (CE) and cellulose acetate (CA) matrices [13], and the same methodology was used in this work, in which, after cutting the structure the ends of the molecules were completed with hydrogen atoms.

To verify the reactivity of complexation between the CMC and CX matrices and the Cu^{2+}, Cd^{2+}, Cr^{3+} metallic ions, the studies of map of electrostatic potential (MEP), frontier molecular orbitals (FMOs) and the reactivity indices were performed. The HOMO, LUMO energies and reactivity indices hardness (η) and softness (S) for adsorption matrices and metallic ions are represented in Table 1. The results were also compared with data previously published by the research group for cellulose acetate and cellulose matrices [13].

The results show that the adsorption matrices CE, CMC and CA present values close to softness, being that CA is relatively softer than CMC which is softer than CE, as shown in Table 1. Ralph Person [35, 36] defined species more polarizable as soft (acid or base) and less polarizable as hard (acid or base). Analyzing the results qualitatively, it is possible to infer that CA presents greater softness because it is more polarizable and this fact can be justified by the resonance that occurs in the substituent. The CMC shows resonance only in the carboxyl group (COOH) and is softer than the CE, which has only hydroxyls.

Table 1 FMOs and reactivity indices hardness (η) and softness (S) for adsorption matrices and metallic ions

Polymer or ion	HOMO	LUMO	(η)	(S)	References
CMC	− 208.352	10.43548	109.3937	0.009141	This work
CX	− 148.776	0.439257	74.60774	0.013403	This work
CA	− 210.473	2.033131	106.253	0.009411	[13]
CE	− 208.703	11.11319	109.9083	0.009098	[13]
Cd^{2+}	− 433.785	34.9711	234.3779	0.004267	[13]
Cu^{2+}	− 75.6525	− 49.749	12.9518	0.077209	[13]
Cr^{3+}	− 214.489	− 202.504	5.992716	0.166869	[13]

Data in kcal mol^{-1}

For metallic ions, Cr^{3+} has the highest softness, followed by Cu^{2+} and finally Cd^{2+}. It can be inferred from the reactivity indices that the softer cation will interact more strongly with the softer polymer according to Pearson's concept where soft interacts with soft and hard interacts with hard [35], but like the CE, CMC and CA have very close values of hardness and softness, and it can be inferred that Cr^{3+} becomes the best candidate for interaction in these three polymers. Comparing CX with the other polymers, it is possible to observe that it is the polymer that presents the greatest softness among all polymers resulting from the negative charge and atomic volume of sulfur. Thus, CX is the polymer that becomes the best candidate for Cr^{3+} adsorption. It is worth mentioning that the values presented in Table 1 are results obtained from the orbitals of Kohn–Sham, as shown in Eqs. 3 and 4.

The chemical structures, MEPs and FMOs are represented in Fig. 1. The MEPs were generated with density 0.001 a.u. More intense color in blue indicates a partially positive region, and the most orange or red color is partially negative region. The metal cations are not shown but as they are positive species, they have a totally blue coloration. Several works of the literature use the analysis of MEPs and show its importance to locate interaction and reaction sites [5, 13].

From the MPEs, as shown in Fig. 1, it is possible to infer that the metallic ions will interact with the oxygen atom of the CMC polymer which have negative charges in the regions where the oxygen is located. In the case of CX, the MEP was modified for the sulfos groups ($–C–S_2^{2-}$) because the sodium atoms (Na) that neutralized the charge were not

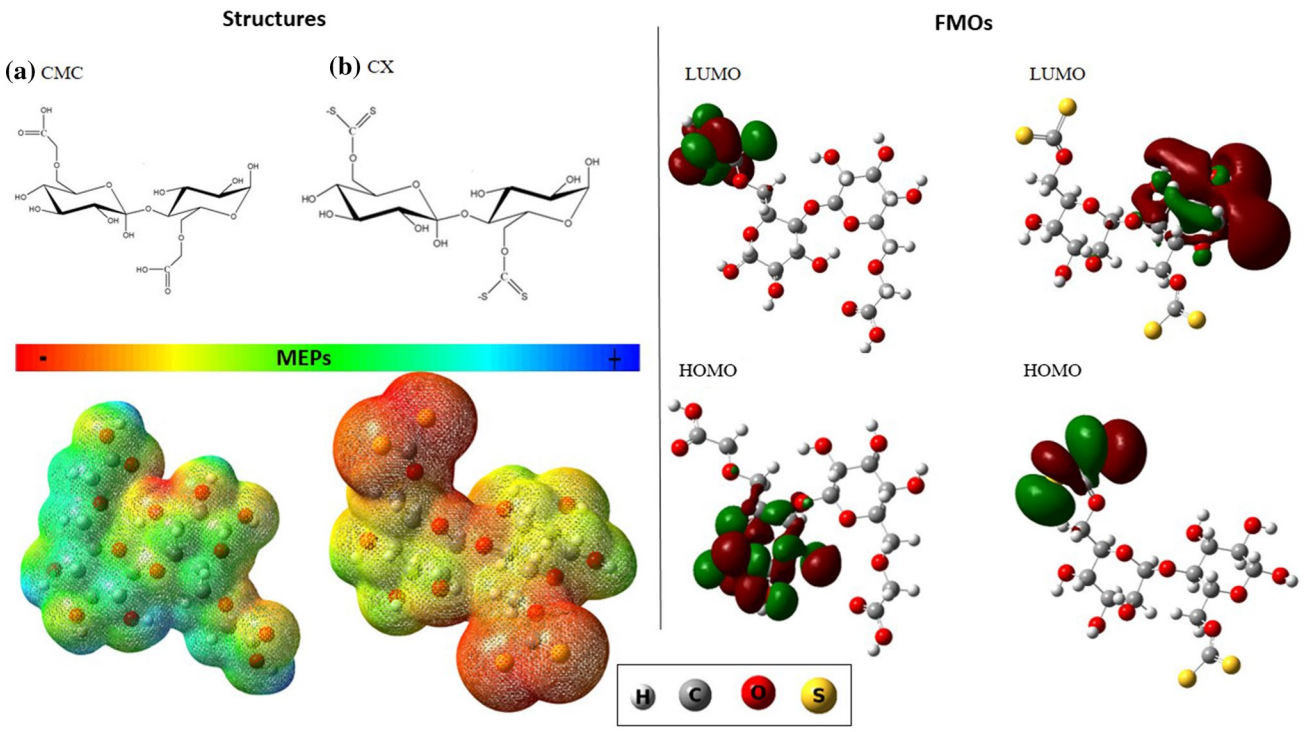

Fig. 1 Structural formula, map of electrostatic potential (MEP), frontier molecular orbitals (FMOs) HOMO and LUMO for: **a** carboxymethylcellulose and **b** cellulose xanthate. The MEPs were generated with density 0.001 a.u and the FMOs with isovalue 0.02

considered in the structure. Na atoms were not considered, because the complexation of ions occurs in aqueous medium and the Na-S bond breaks down releasing Na^+ leaving the negatively charged sulfur (S^-). Thus, from Fig. 1, it is possible to infer that the metal ions will interact with sulfos groups and also with oxygen atoms of the CX.

From the position of the frontier molecular orbitals found for the CMC and CX, as shown in Fig. 1, it is possible to indicate that possibly the metal ions will interact with the oxygen atom of the CMC polymer terminal groups, because the oxygen presents π orbitals that can interact with the metallic ions. In the case of CX, very characteristic π orbitals are observed over the sulfos groups, so this would be the other interaction site. The atomic orbitals (AO) of Cr^{3+}, Cu^{2+} and Cd^{2+} are not represented in Fig. 1 because the species are electropositive and have type d orbitals and the LUMO orbitals of the cations will interact with the HOMO orbitals of matrices that have electrons.

For the complexation study, only the sites described by the analyses of reactivity indices, MEPs and FMOs were evaluated because the analyses adequately predict the location of the interaction. Another point is that the left and right sides of the polymer were not evaluated as a possible site of interaction because the polymer increases in that direction.

3.2 Complex structures

3.2.1 Structural and vibrational analysis

Analyses of MPEs, FMOs and reactivity indices provide information about interaction sites and allowed to reduce the computational cost by directly locating the most probable site. Based on these results, it was decided to locate the metal ions with the hydroxyl (–OH) and carbonyl (–C=O) terminal groups of the CMC. For CX, two interaction sites were analyzed: (1) hydroxyl and sulfo group (–CS) interactions "a" and "b" and the other only about sulfo group ($–C–S_2^{2-}$) with interactions "c" and "d." The optimized structures are represented in Fig. 2 with their respective interactions.

The structural parameters of complex formation are shown in Table 2 with their respective bond distances and vibrational frequencies. For CMC polymer, it is possible to observe that Cr^{3+} ion is the metal that most closely approximates the interaction matrices with values of 2.14 and 2.07 Å for positions "a" and "b," respectively. For CMC complexes, it is also important to note that there are three interactions "a," "b" and "c" with the Cd^{2+} atom. This fact indicates that in the molecule, the three sites compete for the cadmium atom.

The structural parameters of the formation of CX complexes with metals show that for the metallic ions at the two interaction sites, the Cu^{2+} is the closest to the interaction matrix with values of 2.05 and 2.33 Å (positions a and b, respectively) for interaction site (1) and with values of 2.48 and 2.5 Å (position c and d, respectively) for interaction site (2). The values of the interaction distance lengths also show that the first interaction site studied has a shorter bonding length between the metal ions than second site. This fact may be justified, because the oxygen atom has a smaller electronic cloud than sulfur atoms, which results in a shorter bond length.

All vibrational frequencies of complexed bonds decrease with interaction as compared to the vibrational frequencies of isolated molecules thus confirming that interaction has occurred.

3.2.2 Gibbs energy and interaction energy

To evaluate the magnitude of the interaction, Gibbs energy (ΔG) and the electronic interaction energy (E_{int}) of the processes were calculated, as shown in Table 3.

Table 3 shows by the ΔG values that the processes occur spontaneously and the high negative values indicate that the adsorption process occurs by chemisorption.

The E_{int} values show the tendency of metal ions to interact with the adsorption matrices. For CMC, the interaction order found was $Cr^{3+} > Cd^{2+} > Cu^{2+}$. Unlike CMC, the CX presented a more effective interaction for the Cu^{2+} ion than for the Cd^{2+} ion and the order of interaction found was $Cr^{3+} > Cu^{2+} > Cd^{2+}$. E_{int} values for CX also show that the two interactions studied at work are possible and practically similar in terms of energy. This fact indicates that CX is an excellent adsorption matrix, as it has more than one effective interaction site.

Comparing the results with those previously reported by our research group for cellulose and cellulose acetate, it is possible to observe that CMC follows the same trend as CE and CA [13]. In general it can be confirmed that both cellulose and CA, CMC and CX derivatives interact with the metallic ions studied from the theoretical point of view, thus allowing experimental studies of these systems with environmental applications.

3.2.3 QTAIM analysis

The topological parameters were evaluated using QTAIM theory, and the complex results for the interactions are shown in Table 4. The properties analyzed were electron density ($\rho(r)$), electron density Laplacian ($\nabla^2\rho(r)$) and total ($H(r)$) energies.

The higher the electron density value ($\rho(r)$) in the bond critical point (BCP), the greater the intensity of the interaction. When the values of $\nabla^2\rho(r)$ and total energy $H(r)$ are positive, the nature of the interaction is electrostatic,

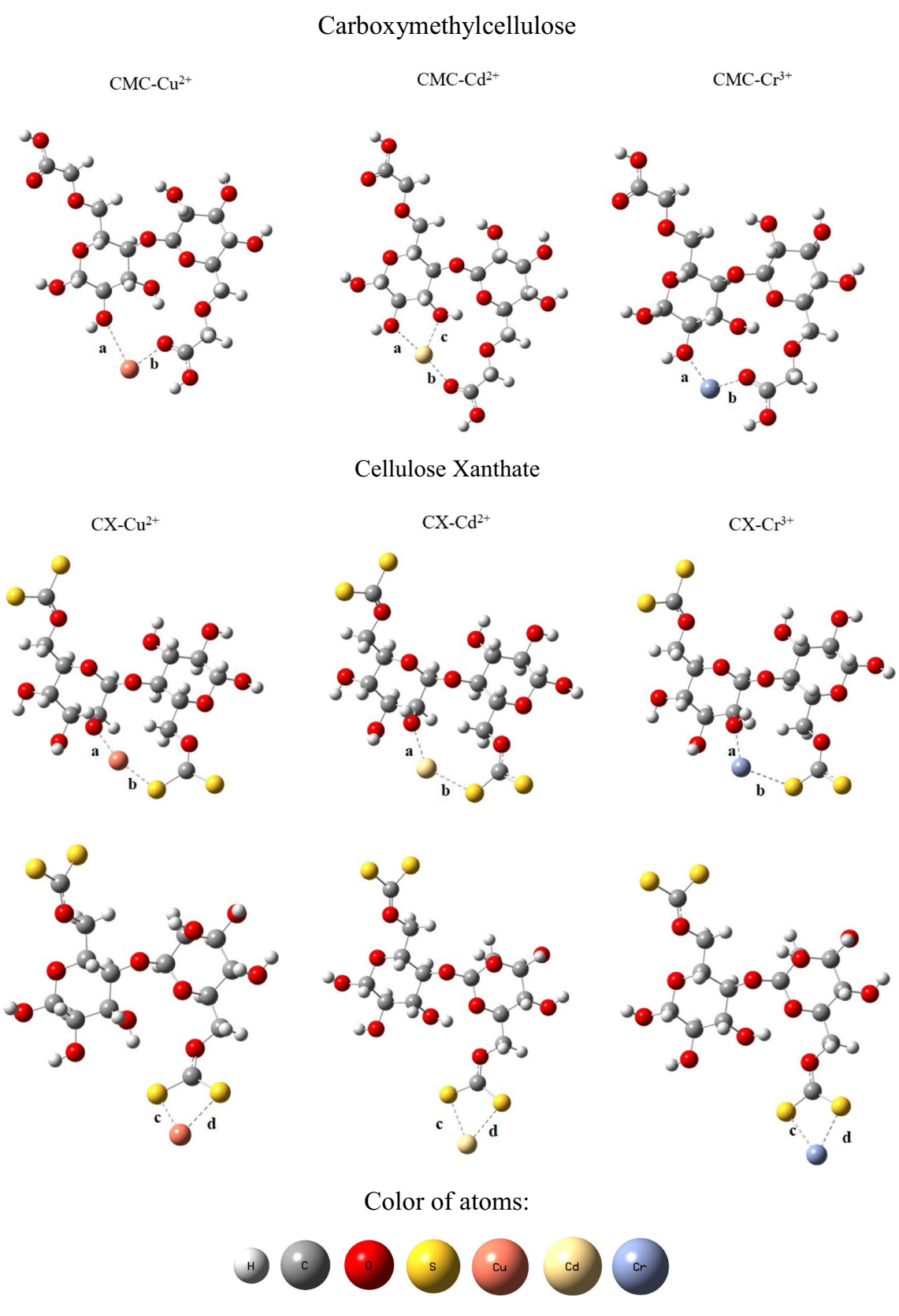

Fig. 2 Optimized structures of CMC and CX interacting with metallic ions Cu^{2+}, Cd^{2+} and Cr^{3+}

Table 2 Calculated interaction distances (in Å) and vibrational frequencies (in cm^{-1}) of carboxymethylcellulose, cellulose xanthate and complexes formed

Molecule/complex	Interaction position	Bonding length	Frequency (infrared data)
CMC	a	–	ν(C–O) 1082.22
	b	–	ν(C=O) 1794.78
	c	–	ν(C–O) 1166.08
CMC–Cu^{2+}	a	2.88	ν(C–O) 1072.27
	b	2.12	ν(C=O) 1748.89
	c	–	–
CMC–Cd^{2+}	a	2.34	ν(C–O) 1065.65
	b	2.31	ν(C=O) 1762.21
	c	2.24	ν(C–O) 1101.66
CMC–Cr^{3+}	a	2.14	ν(C–O) 1070.82
	b	2.07	ν(C=O) 1757.88
	c	–	–
CX	a	–	ν(C–O) 1171.87
	b	–	ν(C=S) 710.67
	c	–	ν(C=S) 710.67
	d	–	ν(C=S) 710.67
CX^1–Cu^{2+}	a	2.05	ν(C–O) 1068.40
	b	2.33	ν(C=S) 710.10
CX^1–Cd^{2+}	a	2.28	ν(C–O) 1171.81
	b	2.65	ν(C=S) 705.77
CX^1–Cr^{3+}	a	2.08	ν(C–O) 1168.67
	b	2.76	ν(C=S) 703.34
CX^2–Cu^{2+}	c	2.48	ν(C=S) 707.82
	d	2.50	ν(C=S) 707.82
CX^2–Cd^{2+}	c	2.72	ν(C=S) 705.35
	d	2.79	ν(C=S) 705.35
CX^2–Cr^{3+}	c	2.58	ν(C=S) 707.61
	d	2.56	ν(C=S) 707.61

[1]Interaction "a" and "b" in Fig. 2 for CX

[2]Interaction "c" and "d" in Fig. 2 for CX

whereas for values of $\nabla^2\rho(r)$ positive and $H(r)$ negative, the interactions are partially covalent. Analyzing $\rho(r)$, it is possible to observe the same trend as E_{int}'s calculations. All interactions are non-covalent because they presented positive electron density Laplacian values ($\nabla^2\rho > 0$).

The results found, as shown in Table 4, show that for CMC, the interactions in position "b" of CMC–Cu^{2+}, CMC–Cd^{2+} and position "a" of CMC–Cd^{2+} complex have positive $\nabla^2\rho(r)$ and positive $H(r)$ evidencing electrostatic characteristics differently from other interactions. The results obtained by QTAIM did not identify the "c" bond of the CMC–Cd^{2+} complex and could not be classified.

For the interactions "a" in the complexes XC–Cu^{2+}, XC–Cd^{2+} and "b" in the XC–Cr^{3+} site 1), the values are positive for $\nabla^2\rho(r)$ and H(r) and therefore have electrostatic character. All other interactions, site 1 and site 2 are partially covalent ($\nabla^2\rho > 0$ and $H(r) < 0$).

Another important point of the topological parameters $\nabla^2\rho(r)$ and $H(r)$ in predicting the nature of the interaction is that it can infer whether the interaction is soft–hard or hard–hard. For an electrostatic interaction, it can be attributed that the interaction is of the hard–hard type, because in this interaction, there is little involvement of the electronic density. However, for partially covalent interactions, it can be said that the interaction is soft–soft, because the electronic density participates more effectively in the interaction. From Table 4, the hard–hard interactions are for the CMC–Cu^{2+} in position "b," CMC–Cd^{2+} in positions "a" and "b," XC^1–Cu^{2+} in position "a," XC^1–Cd^{2+} in position "a" and XC^1–Cr^{3+} in position "b." For the other interactions, the interactions are soft–soft.

4 Conclusion

Therefore, the results obtained to provide insight into the use of carboxymethylcellulose and cellulose xanthate for the removal of Cr^{3+}, Cu^{2+} and Cd^{2+} of effluents. By calculating reactivity indices, MEPs and FMOs, it was possible

Table 3 Electronic interaction energy (E_{int}) at 0 Kelvin and Gibbs energy (ΔG) at 298 K for the studied complexes

	Interaction energy			Gibbs energy			References
	Cu^{2+}	Cd^{2+}	Cr^{3+}	Cu^{2+}	Cd^{2+}	Cr^{3+}	
CMC	−110.1628	−432.9838	−1064.7365	−100.9845	−424.6300	−1056.3056	This work
CX^1	−228.3181	−141.1338	−1146.3643	−219.7664	−134.1270	−1136.8652	This work
CX^2	−226.0001	−144.9892	−1111.9995	−218.2540	−148.4951	−1113.4233	This work
CE	−117.8349	−429.6905	−1070.0523	−109.8788	−421.0087	−1059.6765	[13]
CA	−99.6148	−418.2926	−1056.7389	−91.4689	−408.9881	−1047.7771	[13]

The values were obtained in aqueous phase with theory level M06-2X/6-31+G(*d*,*p*)/LANL2DZ. Data in kcal mol^{-1}

[1]Interaction "a" and "b" in Fig. 2 for CX

[2]Interaction "c" and "d" in Fig. 2 for CX

Table 4 Topological parameters calculated in atomic units (a.u.) in the selected BCPs

Complex	Interaction	$\rho(r)$	$\nabla^2\rho(r)$	H(r)
CMC–Cu^{2+}	a	0.011	0.021	−0.002
	b	0.041	0.211	0.004
CMC–Cd^{2+}	a	0.008	0.019	0.001
	b	0.054	0.281	0.000
	c	–	–	–
CMC–Cr^{3+}	a	0.056	0.281	−0.002
	b	0.062	0.335	−0.002
CX^1–Cu^{2+}	a	0.058	0.444	0.010
	b	0.064	0.225	−0.006
CX^1–Cd^{2+}	a	0.051	0.269	0.000
	b	0.046	0.114	−0.006
CX^1–Cr^{3+}	a	0.064	0.389	−0.005
	b	0.027	0.102	0.001
CX^2–Cu^{2+}	c	0.045	0.161	−0.002
	d	0.044	0.157	−0.002
CX^2–Cd^{2+}	c	0.042	0.095	−0.005
	d	0.036	0.086	−0.003
CX^2–Cr^{3+}	c	0.041	0.155	−0.003
	d	0.042	0.160	−0.004

[1]Interaction "a" and "b" in Fig. 2 for CX

[2]Interaction "c" and "d" in Fig. 2 for CX

to locate the best interaction site of the adsorption matrix with the studied metallic ions. The results found in the work showed that among the studied matrices, the CX is the one that has the greatest interaction potential because it has two complexation sites. In general, for all matrices, the Cr^{3+} ion is the metal ion that best interacts with the matrices and all interactions are chemisorption and spontaneous. The QTAIM analyses showed that the interactions in position "b" of CMC–Cu^{2+}, CMC–Cd^{2+} and position "a" of CMC–Cd^{2+} and "a" in the complexes XC–Cu^{2+}, XC–Cd^{2+} and "b" in the XC–Cr^{3+} site (1) presented electrostatic character and the other interactions were partially covalent. Finally, it is possible to infer that the results for carboxymethylcellulose and cellulose xanthate corroborate those reported in the literature by our research group for cellulose matrices and cellulose acetate.

Acknowledgements The authors acknowledge funding from CAPES (Coordination of Improvement of Higher Education Personnel—Brazil), Funding Code 001 CAPES. Pereira DH acknowledges the Center for Computational Engineering and Sciences (Financial support from FAPESP Fundação de Amparo à Pesquisa, Grant 2013/08293-7, and Grant 2017/11485-6), the National Center for High Performance Processing (Centro Nacional de Processamento de Alto Desempenho—CENAPAD) in São Paulo and UNICAMP (Universidade Estadual de Campinas), for computational resources.

References

1. de Oliveira Barud HG, da Silva RR, da Silva Barud H et al (2016) A multipurpose natural and renewable polymer in medical applications: bacterial cellulose. Carbohydr Polym 153:406–420. https://doi.org/10.1016/j.carbpol.2016.07.059
2. Lebedeva NSh, Guseinov SS, Yurina ES et al (2019) Thermochemical research of chitosan complexes with sulfonated metallophthalocyanines. Int J Biol Macromol 137:1153–1160. https://doi.org/10.1016/j.ijbiomac.2019.07.051
3. Pereira AKDS, Reis DT, Barbosa KM et al (2020) Antibacterial effects and ibuprofen release potential using chitosan microspheres loaded with silver nanoparticles. Carbohydr Res 488:107891. https://doi.org/10.1016/j.carres.2019.107891
4. Van de Velde K, Kiekens P (2002) Biopolymers: overview of several properties and consequences on their applications. Polym Test 21:433–442. https://doi.org/10.1016/S0142-9418(01)00107-6
5. Reis DT, Pereira AKDS, Scheidt GN, Pereira DH (2019) Plant and bacterial cellulose: production, chemical structure, derivatives and applications. Orbital Electron J Chem 11:321–329. https://doi.org/10.17807/orbital.v11i5.1349
6. Ribeiro IHS, Reis DT, Pereira DH (2019) A DFT-based analysis of adsorption of Cd^{2+}, Cr^{3+}, Cu^{2+}, Hg^{2+}, Pb^{2+}, and Zn^{2+}, on vanillin monomer: a study of the removal of metal ions from effluents. J Mol Model 25:267. https://doi.org/10.1007/s00894-019-4151-z
7. Kanmani P, Aravind J, Kamaraj M et al (2017) Environmental applications of chitosan and cellulosic biopolymers: a comprehensive outlook. Bioresour Technol 242:295–303. https://doi.org/10.1016/j.biortech.2017.03.119
8. Ren N-Q, Zhao L, Chen C et al (2016) A review on bioconversion of lignocellulosic biomass to H2: key challenges and new insights. Bioresour Technol 215:92–99. https://doi.org/10.1016/j.biortech.2016.03.124
9. Rajeswari A, Amalraj A, Pius A (2016) Adsorption studies for the removal of nitrate using chitosan/PEG and chitosan/PVA polymer composites. J Water Process Eng 9:123–134. https://doi.org/10.1016/j.jwpe.2015.12.002
10. An B, Jung K-Y, Zhao D et al (2014) Preparation and characterization of polymeric ligand exchanger based on chitosan hydrogel for selective removal of phosphate. React Funct Polym 85:45–53. https://doi.org/10.1016/j.reactfunctpolym.2014.10.003
11. Isik M, Sardon H, Mecerreyes D (2014) Ionic liquids and cellulose: dissolution, chemical modification and preparation of new cellulosic materials. Int J Mol Sci 15:11922–11940. https://doi.org/10.3390/ijms150711922
12. Silva Filho EC, Santos Júnior LS, Silva MMF et al (2013) Surface cellulose modification with 2-aminomethylpyridine for copper, cobalt, nickel and zinc removal from aqueous solution. Mater Res 16:79–84. https://doi.org/10.1590/S1516-14392012005000147
13. Reis DT, Ribeiro IHS, Pereira DH (2019) DFT study of the application of polymers cellulose and cellulose acetate for adsorption of metal ions (Cd^{2+}, Cu^{2+} and Cr^{3+}) potentially toxic. Polym Bull. https://doi.org/10.1007/s00289-019-02926-5
14. Liang S, Guo X, Feng N, Tian Q (2010) Effective removal of heavy metals from aqueous solutions by orange peel xanthate. Trans Nonferr Met Soc China 20:s187–s191. https://doi.org/10.1016/S1003-6326(10)60037-4
15. Beyki MH, Bayat M, Miri S et al (2014) Synthesis, Characterization, and silver adsorption property of magnetic cellulose xanthate from acidic solution: prepared by one step and biogenic approach. Ind Eng Chem Res 53:14904–14912. https://doi.org/10.1021/ie501989q

16. Biswal DR, Singh RP (2004) Characterisation of carboxymethyl cellulose and polyacrylamide graft copolymer. Carbohydr Polym 57:379–387. https://doi.org/10.1016/j.carbpol.2004.04.020
17. Siegel FR (2002) Environmental geochemistry of potentially toxic metals. Springer, Berlin
18. Castagnetto JM, Hennessy SW, Roberts VA et al (2002) MDB: the metalloprotein database and browser at the scripps research institute. Nucl Acids Res 30:379–382. https://doi.org/10.1093/nar/30.1.379
19. Nascimento RF do, Lima ACA de, Vidal CB et al (2014) Adsorção: aspectos teóricos e aplicações ambientais. Impresso no Brasil. Ceará
20. do Nascimento RF, Sousa Neto VDO, Melo DDQ (2014) Uso de bioadsorventes lignocelulósicos na remoção de poluentes de efluentes aquosos. Impresso no Brasil. Ceará
21. Rehman K, Fatima F, Waheed I, Akash MSH (2018) Prevalence of exposure of heavy metals and their impact on health consequences. J Cell Biochem 119:157–184. https://doi.org/10.1002/jcb.26234
22. Galaris D, Evangelou A (2002) The role of oxidative stress in mechanisms of metal-induced carcinogenesis. Crit Rev Oncol/Hematol 42:93–103. https://doi.org/10.1016/S1040-8428(01)00212-8
23. Monalisa M, Kumar PH (2013) Effect of ionic and chelate assisted hexavalent chromium on mung bean seedlings (*Vigna radiata* L, wilczek, Var k-851) during seedling growth. J Stress Physiol Biochem, vol 9. https://cyberleninka.ru/article/n/effect-of-ionic-and-chelate-assisted-hexavalent-chromium-on-mung-bean-seedlings-vigna-radiata-l-wilczek-var-k-851-during-seedling-growth
24. Rodríguez MC, Barsanti L, Passarelli V et al (2007) Effects of chromium on photosynthetic and photoreceptive apparatus of the alga *Chlamydomonas reinhardtii*. Environ Res 105:234–239. https://doi.org/10.1016/j.envres.2007.01.011
25. Zhao Y, Truhlar DG (2008) The M06 suite of density functionals for main group thermochemistry, thermochemical kinetics, noncovalent interactions, excited states, and transition elements: two new functionals and systematic testing of four M06-class functionals and 12 other functionals. Theor Chem Acc 120:215–241. https://doi.org/10.1007/s00214-007-0310-x
26. Marenich AV, Cramer CJ, Truhlar DG (2009) Universal solvation model based on solute electron density and on a continuum model of the solvent defined by the bulk dielectric constant and atomic surface tensions. J Phys Chem B 113:6378–6396. https://pubs.acs.org/doi/abs/10.1021/jp810292n
27. Frisch MJ, Trucks GW, Schlegel HB, Scuseria GE, Robb M A, Cheeseman JR, Scalmani G, Barone V, Petersson GA, Nakatsuji H, Li X, Caricato M, Marenich AV, Bloino J, Janesko BG, Gomperts R, Mennucci B, Hratchian HP, Ortiz JV, Izmaylov AF, Sonnenberg JL, Williams-Young D, Ding F, Lipparini F, Egidi F, Goings J, Peng B, Petrone A, Henderson T, Ranasinghe D, Zakrzewski VG, Gao J, Rega N, Zheng G, Liang W, Hada M, Ehara M, Toyota K, Fukuda R, Hasegawa J, Ishida M, Nakajima T, Honda Y, Kitao O, Nakai H, Vreven T, Throssell K, Montgomery JA Jr, Peralt, JE, Ogliaro F, Bearpark MJ, Heyd JJ, Brothers EN, Kudin KN, Staroverov VN, Keith TA, Kobayashi R, Normand J, Raghavachari K, Rendell AP, Burant JC, Iyengar SS Tomasi J, Cossi M, Millam JM, Klene M, Adamo C, Cammi R, Ochterski JW, Martin RL, Morokuma K, Farkas O, Foresman JB, Fox DJ (2016) Gaussian 09, Revision C.01. Gaussian, Inc, Wallingford
28. Dennington R, Keith T, Millam J (2009) GaussView, Version 5. Semichem Inc, Shawnee Mission
29. Koopmans T (1934) Über die Zuordnung von Wellenfunktionen und Eigenwerten zu den Einzelnen Elektronen Eines Atoms. Physica 1:104–113. https://doi.org/10.1016/S0031-8914(34)90011-2
30. Bader RFW, Essén H (1984) The characterization of atomic interactions. J Chem Phys 80:1943–1960. https://doi.org/10.1063/1.446956
31. Keith TA, Bader RFW, Aray Y (1996) Structural homeomorphism between the electron density and the virial field. Int J Quantum Chem 57:183–198. https://doi.org/10.1002/(SICI)1097-461X(1996)57:2%3c183:AID-QUA4%3e3.0.CO;2-U
32. Kumar PSV, Raghavendra V, Subramanian V (2016) Bader's theory of atoms in molecules (AIM) and its applications to chemical bonding. J Chem Sci 128:1527–1536. https://doi.org/10.1007/s12039-016-1172-3
33. Popelier PLA (1999) Quantum molecular similarity, 1, BCP space. J Phys Chem A 103:2883–2890. https://doi.org/10.1021/jp984735q
34. Keith TA (2017) AIMAll (Version 17.11.14). TK Gristmill Software, Overland Park KS, USA (aim.tkgristmill.com)
35. Pearson RG (1963) Hard and soft acids and bases. J Am Chem Soc 85:3533–3539. https://pubs.acs.org/doi/abs/10.1021/ja00905a001
36. Vasconcellos MLAA (2014) A teoria de pearson para a disciplina de Química Orgânica: um exercício prático e teórico aplicado em sala de aula. Quím Nova 37(1):171–175. https://doi.org/10.1590/S0100-40422014000100029